Proceedings of the 21st ICSMGE, Vienna, Austria, 14 – 19 June 2026. Pistrol, Adam & Schweiger (eds.)
Published by: ÖGG, Austrian Society for Geomechanics, Salzburg, Austria, ISBN 978-3-9503898-4-5
https://doi.org/10.53243/ICSMGE2026-570

Numerical modelling of a deep excavation in the overconsolidated soil of Vienna

Aleksandar Kostadinovic, Julian Sigmund, Dietmar Adam
Institute of Geotechnics, TU Wien, Austria, aleksandar.kostadinovic@tuwien.ac.at

ABSTRACT: This contribution deals with the numerical modeling of a 33-meter-deep excavation in the overconsolidated soil of Vienna. Diaphragm walls are used as retaining structures, which are integrated into the newly constructed metro station at Matzleinsdorfer Platz. Due to deformation-sensitive buildings in the vicinity of the shaft, a comprehensive deformation monitoring system had to be installed on the site. Numerical 2D- and 3D-models, based on the finite element method, were created and compared with each other. Among other approaches, elastoplastic material models with isotropic hardening (Hardening Soil Model with and without small strain stiffness) were used. The soil stiffness parameters of the Hardening Soil Model have been determined through laboratory and field tests. Due to the low hydraulic permeability of the soil, the study also explores the impact of various drainage conditions (drained, undrained, consolidation) on the deformation behavior of the shaft, resulting in a set of 24 calculation models. The calculated deformations are compared with the in-situ measurements of the actual shaft to validate the used soil stiffness parameters and material models. Following a detailed analysis of the results, a suitable calculation model is selected for further soil parameter and sensitivity studies. In the soil parameter study, the effect of the pre-consolidation pressure of the overconsolidated miocene soil layers on the deformation of the diaphragm walls and excavation base is analyzed by varying the pre-overburden pressure (POP) in the calculation model. Additionally, assuming the soil parameters follow a normal distribution, shear and stiffness parameters are varied based on standard deviations from literature. The sensitivity study further explores the influence of the diaphragm wall thickness and concrete beam prop width on the deformation behavior of the retain walls and the basal heave.

KEYWORDS: Deep Excavation, Finite Element Analysis, Hardening Soil Model, Numerical Modelling, Parameter Study.

1 INTRODUCTION

The Finite Element Method (FEM) has become the dominant numerical calculation method in structural engineering (Bode et al., 2019). In geotechnical engineering, particularly in Austria, numerical methods are increasingly being applied. However, they have not yet become standard practice. This is largely due to the absence of clear national regulations or standardized guidelines regarding numerical modelling and verification procedures. Although Eurocode 7 (European Committee for Standardization, 2014) permits the use of numerical methods, it offers little guidance on model formulation and validation. Consequently, engineers often need to consult supplementary literature (Deutsche Gesellschaft für Geotechnik, 2014).

Geotechnical problems are inherently complex and traditional analytical methods often have their limitations. Such methods usually require significant simplifications and assumptions regarding soil behavior, such as the pre-definition of slip surfaces in slope stability analysis or the use of idealized earth pressure distributions in retaining wall design. By contrast, numerical methods such as finite element analysis (FEA) allow failure mechanisms to emerge naturally within the simulation framework, thereby reducing the need for predefined assumptions (Kostadinovic et al., 2024).

Unlike in structural engineering, where standardized material models are often sufficient, there is no universally applicable constitutive model for soils. A suitable soil model must be selected based on the specific problem and the characteristics of the soil involved. One widely used model for deformation analysis is the Hardening Soil (HS) model, which is an elastoplastic constitutive model that incorporates isotropic hardening (Schanz, 1998). A distinguishing feature of the HS model is its use of stress-dependent and stress-path-dependent stiffness parameters. These parameters enable differentiation between loading, unloading and reloading behaviors based on the specific stress history and loading conditions. The HS model is particularly suited for excavation-related deformation analyses, such as those involving retaining walls and tunnels (Deutsche Gesellschaft für Geotechnik, 2014). To enhance its accuracy, particularly under small-strain conditions that are critical to many geotechnical applications, the Hardening Soil model with small-strain stiffness (HSS model) was developed. This extended model accounts for the increased stiffness of soils at very low strain levels – an effect often overlooked in standard laboratory tests, yet which is crucial for accurate deformation predictions, particularly in deep excavations and retaining systems (Benz et al., 2007; Hardin and Drnevich, 1972).

This study examines how different constitutive models, drainage conditions and soil stiffness parameters affect the results of finite element simulations. The case study focuses on a deep diaphragm wall shaft located in the overconsolidated soil of Vienna. Numerical modelling and subsequent deformation analyses were conducted using Plaxis 2D and 3D (version 2023.1). The performance of both the HS and HSS models were compared for two different sets of soil parameters. The first set of soil parameters was derived from in situ self-drilling pressuremeter tests, which provide stiffness values that closely represent the behavior of the soil in its natural state. The second set was based on conventional laboratory tests performed on extracted soil samples. The simulation results were validated using field measurements obtained from the constructed shaft. Wall deformations were compared with inclinometer measurements, while basal heave of the shaft is verified using extensometers, hose levels, and geodetic leveling (Kostadinovic, 2023).

Recent research supports the conclusion that incorporating the small-strain stiffness effect into finite element method (FEM) models significantly improves the reliability of deformation predictions for deep excavations. The Hardening Soil model with small-strain stiffness has been validated by numerous case studies, which have compared calculated deformations with actual measurement data from deep excavations (Benz, 2007; Bode et al., 2019; Burd et al., 2016; Chowdhury et al., 2013; Dong et al., 2015; Houhou et al., 2019; Law et al., 2014; Schweiger et al., 2009; Zhang and Liu, 2022). Based on such studies, a broad range of recommendations for numerical modelling in geotechnical engineering has emerged. These include considerations of the anisotropic behavior of diaphragm walls (Klein and Moormann, 2017; Zdravkovic et al., 2005), interaction between soil and structural elements (Ampera and Aydogmus, 2005; Potyondy, 1961), and the

influence of overconsolidation in fine-grained soils (Melnikov et al., 2016).

2 DESCRIPTION OF THE CONSTRUCTION PROJECT "SCHACHT TRIESTER STRASSE"

The shaft "Triester Straße" is a crucial part of the construction of the new subway line U5 in Vienna. It was constructed using the top-down method, with the excavation enclosed by a 1,20 m thick diaphragm wall. The pit has a nearly parallelogram-shaped floor plan, measuring approximately 65 m by 35 m, with an excavation depth of about 33 m (Figure 1).

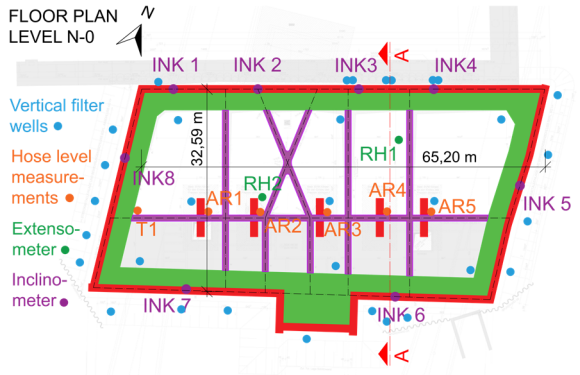

Figure 1. Floor plan level N-0 (Kostadinovic, 2023).

Four bracing levels were installed at horizons N-0, N-2, N-3, and N-4. The lowest level, N-4, consisted of a temporary steel strut system that was removed after the base slab was constructed. In the center of the shaft, freestanding diaphragm wall slats were built to serve as temporary pillars supporting the bracing beams. A reinforced concrete beam runs longitudinally across the shaft, connecting all the transverse bracing beams, which is supported by the temporary central pillars. To compensate for the heave of these central pillars during excavation, the longitudinal concrete beam was supported by a height-adjustable hydraulic jacking system.

The subsoil conditions at the site are primarily defined by Miocene deposits of the Vienna Basin overlain by Pleistocene terrace gravels (Figure 2). The Miocene layers, also referred to as "Wiener Tegel", consist of overconsolidated clayey silts. During construction, vertical filter wells were installed inside and outside the shaft to lower the groundwater table (Kostadinovic, 2023).

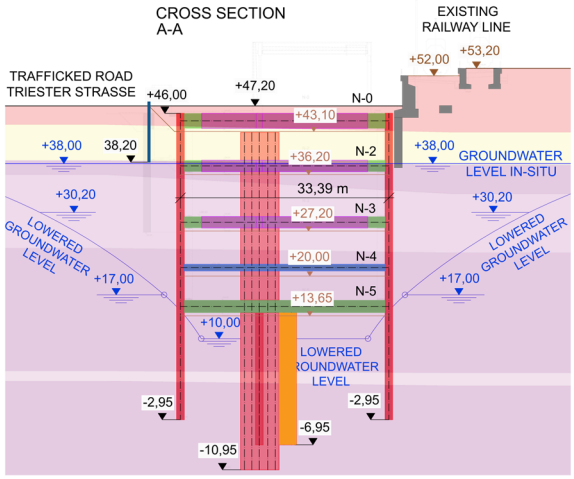

Figure 2. Cross section A-A (Kostadinovic, 2023).

Eight vertical inclinometers were embedded in the shaft's outer diaphragm walls to monitor the horizontal deformations of the diaphragm walls. The heave of the central pillars was measured continuously using hose levels installed at floor level N-2, supplemented by geodetic leveling at designated measurement points (AR1 to AR5). Additionally, two chain extensometers (RH1 and RH2) were used to monitor heave at different depths of the excavation base (Kostadinovic, 2023).

3 NUMERICAL MODELLING OF THE SHAFT

The numerical modeling of the shaft was carried out using the finite element software Plaxis 2D and 3D (version 2023.1). The soil stiffness parameters for the Hardening Soil (HS) model were defined using two different data sources for the Miocene soil layers. The lower bound of the stiffness parameters was based on conventional laboratory tests of soil samples (referred to as Set 2), and the upper bound was derived from in situ self-drilling pressuremeter tests (referred to as Set 1). The HSS model requires small-strain stiffness parameters: the initial shear modulus G_0 and the threshold shear strain $\gamma_{0,7}$. These parameters were estimated using the available empirical correlations in the literature (Benz et al., 2007; Biarez and Hicher, Stokoe et al., 2004; Vucetic and Dobry, 1991; Wichtmann and Triantafyllidis, 2006). Further details on the derivation of these parameters can be found in Kostadinovic (2023). A summary of both parameter sets is provided in Table 1.

Table 1. Soil Parameter Set 1 (field tests) and Soil Parameter Set 2 (laboratory tests) of the Miocene soil layers (Kostadinovic, 2023).

Symbol	Unit	Miocene (Set 1)	Miocene (Set 2)
γ_{unsat}	kN/m³	20,0	20,0
γ_{sat}	kN/m³	20,5	20,5
γ'	kN/m³	10,5	10,5
E_{50}^{ref}	kN/m²	20 000	10 000
E_{oed}^{ref}	kN/m²	25 000	10 000
E_{ur}^{ref}	kN/m²	100 000	40 000
m	-	0,80	0,80
p_{ref}	kN/m²	100	100
ν_{ur}	-	0,20	0,20
G_0^{ref}	kN/m²	120 000	80 000
$\gamma_{0,7}$	-	4E-04	4E-04
c'	kN/m²	30	30
φ'_{HS}	°	25	25
ψ	°	0	0
R_{inter}	-	0,90	0,90
K_0	-	0,75	0,75
K_0^{NC}	-	0,58	0,58
POP	kN/m²	800	800

In the 2D model, the diaphragm walls and base slab were modeled as linear-elastic, isotropic plate elements. The bracing beams and temporary steel struts were modeled with node-to-node anchors. The temporary central pillars, which were constructed as freestanding diaphragm wall slats, were modeled as embedded beam elements (square piles) connected by rigid links. To simulate soil-structure interaction via interface elements, a reduction factor (R_{inter}) must be specified. For the Miocene soils, this factor was assumed between 0,80 and 1,00, according to the findings of Potyondy (1961).

In the 3D model, the diaphragm wall was modeled with anisotropic material behavior. The walls were modeled as plate elements with cross-anisotropic, linear-elastic properties, which allowed for distinct stiffness in the longitudinal and

transverse directions. To account for a reduction in stiffness along the excavation's longitudinal axis, a reduction factor of $\alpha = 0{,}65$, as proposed by Klein and Moormann (2017), was applied to the moment of inertia ($EI_z = 0{,}65 \cdot EI_y$). The connections between the outer diaphragm walls at the corners of the shaft were modeled rigid based on the findings of Zdravkovic (2005). The concrete bracing beams were modeled as beam elements and the temporary steel struts at level N-4 were modeled as node-to-node anchors. Groundwater conditions were defined by a reconstructed drawdown funnel, based on measured groundwater levels and the positions of vertical filter wells installed during the construction phase (see Figures 1 and 2) (Kostadinovic, 2023).

4 ANALYSIS AND INTERPRETATION OF THE CALCULATION RESULTS

A total of 24 calculation models were created in the course of the numerical analyses. The models differ in terms of material models (HS/HSS), model dimensions (2D/3D), soil parameter sets (Set 1 from in situ tests or Set 2 from laboratory tests), and drainage conditions (drained, undrained, or consolidation).

4.1 *Horizontal deformation of the diaphragm wall*

To validate the calculated diaphragm wall deformations, inclinometer data from measurement point INKL 3 were used. These measurements were obtained after the temporary steel struts at level N-4 were removed. The resultant horizontal deformation from the inclinometer was used for comparison, which allows for a valid evaluation even in cases of twisted inclinometer tube installation. Displacements parallel to the wall are assumed to be negligible. Therefore, the measured wall deformations are interpreted as displacements perpendicular to the diaphragm wall.

The inclinometer tubes do not extend to the toe of the diaphragm wall, they end approximately 7 meters above the wall´s toe (see Figure 3). To enable a full-profile comparison, the measured displacement curve was extended by an estimated toe displacement. This estimation corresponds to the calculated toe movement from the consolidation analysis using the 3D-HSS model with Soil Parameter Set 2 which provided the best match with the measured data, and serves as a proxy for the unmeasured translational movement of the diaphragm wall.

Table 2. Comparison of the diaphragm wall deformation between the adapted inclinometer measurement from inclinometer 3 and the calculation results (Kostadinovic, 2023).

Horizontal diaphragm wall deformations (inclinometer 3) Comparison between the adapted inclinometer measurement result and the calculation results Adapted reference horizontal deformation from inclinometer measurement $u_{h,max}$ = 40mm					
Model Configuration				**Calculation result $u_{h,max}$ [mm]**	**Deviation from adapted inclinometer measurement [%]**
Consolidation	HSS	Set 1	3D	32	-19%
			2D	44	11%
		Set 2	**3D**	**41**	**3%**
			2D	53	34%
	HS	Set 1	3D	52	29%
			2D	62	55%
		Set 2	3D	102	155%
			2D	95	137%
Undrained	HSS	Set 1	3D	26	-35%
			2D	49	22%
		Set 2	3D	33	-18%
			2D	62	56%
	HS	Set 1	3D	46	16%
			2D	65	62%
		Set 2	3D	79	98%
			2D	104	159%
Drained	HSS	Set 1	3D	42	5%
			2D	70	76%
		Set 2	3D	54	36%
			2D	91	127%
	HS	Set 1	3D	64	60%
			2D	93	133%
		Set 2	3D	120	201%
			2D	140	250%

Of all the model configurations, the 3D-HSS model with Set 2 (based on laboratory tests) produced the greatest agreement with the inclinometer measurements (pink solid line in Figure 3). The influence of small-strain stiffness is evident, as it significantly affects the wall's horizontal deformation behavior. As expected, the impact of this effect decreases as the HS model's stiffness parameters increase. For example, the 3D-HS model with Set 2 calculated deformations up to 149 % greater than the 3D-HSS model with the same parameter set.

A comparison of the drainage conditions reveals that the drained analysis leads to up to 70 % greater deformations than the consolidation analysis. Conversely, undrained analyses show divergent results: with 3D models, deformations are up to 22 % lower than in the consolidation case, whereas 2D models show deformations up to 17 % higher. This discrepancy is attributed to the plane strain assumption in 2D analyses, which restricts out-of-plane deformations and forces the model to accommodate volume-constant deformation within the plane, resulting in overestimated displacements.

When comparing the influence of soil parameter sets, Set 1 (field-derived parameters) results in smaller deformations than Set 2 (laboratory-based) across all model configurations. In HSS models, the differences range between 17 % and 23 %, while in HS models, they range between 34 % and 49 %. The smaller deviations observed in HSS models are attributed to their higher initial stiffness at small strains (Kostadinovic, 2023).

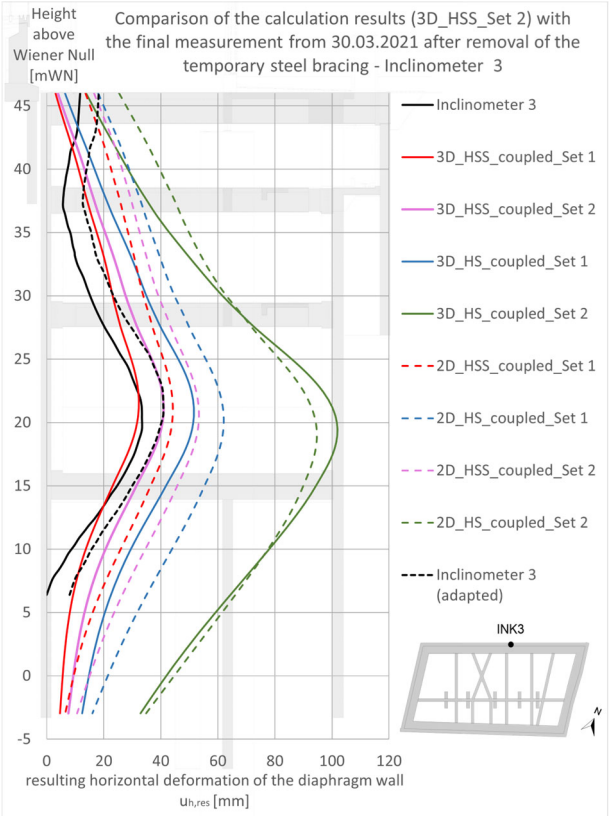

Figure 3. Deformation of the diaphragm wall at inclinometer 3; comparison between the inclinometer data and the calculation results from the consolidation (coupled) analysis (Kostadinovic, 2023).

In general, 3D models predict larger wall displacements than 2D models (see Table 2). This difference is due to the spatial modeling in 3D, which captures effects such as corner stiffness and spatial stress redistribution. These effects are neglected in 2D models because of their simplified plane strain formulation.

4.2 *Heave of the excavation base*

The heave of the excavation base was evaluated by comparing measured vertical displacements recorded by chain extensometers with calculated elevations obtained from various numerical model configurations. Because extensometer measurements are interpreted relative to the anchor point, the heave at the anchor location must be subtracted from the computed absolute displacement at each measurement point to enable reasonable comparison.

The best match with the extensometer data was achieved using the 3D-HSS model with Soil Parameter Set 2. Figure 4 compares the measured basal heave at measurement point RH 1.4 with the numerical results from drained, undrained, and consolidation analyses.

The consolidation and undrained analyses closely replicate the measured heave. However, the drained analysis results in significant discrepancies, particularly in the form of early settlements. This confirms the assumption that fully drained conditions were not present during construction (Kostadinovic, 2023).

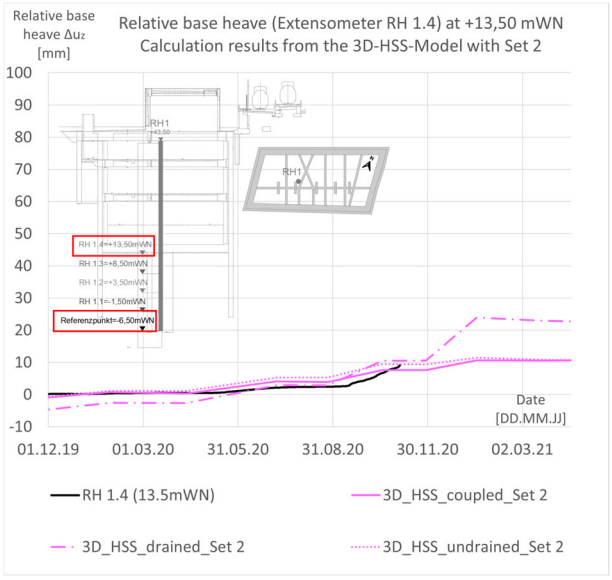

Figure 4. Comparison of calculated relative basal heaves from the 3D-HSS model using Set 2 with the measurements from Extensometer RH 1.4 (Kostadinovic, 2023).

The greatest heave of the excavation base was measured at measurement point RH 2.4, which corresponds to the anticipated location of the maximal heave that can occur due to the formation of an elevation vault. Figure 5 shows the consolidation analysis results for all model configurations. The 2D models (dashed lines) consistently calculate larger heaves than the 3D models, due to their inability to capture spatial effects, such as the formation of soil arching effects.

The influence of small-strain stiffness is evident: models using the HS formulation (green and blue solid lines) calculate greater heave than models using the HSS formulation (red and pink solid lines). The HSS-based simulations consistently yield lower heave values, with deviations from the HS model reaching up to 385 %. As the soil stiffness parameters in the HS model increase, the effect of small-strain stiffness decreases (Kostadinovic, 2023).

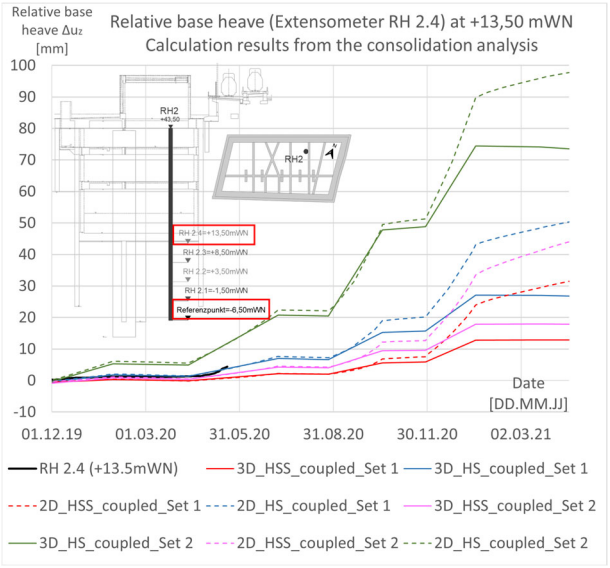

Figure 5. Relative basal heave around Extensometer RH 2.4; comparison between the measured data and the calculation results from the consolidation analysis (Kostadinovic, 2023).

4.3 *Heave of the temporary central pillar*

To evaluate the vertical displacement of the temporary central pillars, the results of the hose level measurements and geodetic leveling at central pillar 3 were compared with the results of the numerical calculations. A distinction was made between relative heave, which was measured by hose level sensor 3 with respect to reference point T1, and absolute heave, which was derived from geodetic measurements at point AR 3.

The HS model with Set 2 (green lines) significantly overestimates the heave. On the other hand, the 3D-HSS model with Set 1 underestimates the measured values (Figure 6). The 3D-HSS model with Set 2 (pink solid line) yields the best agreement between measurements and simulation. Though minor local deviations occur, the consolidation analysis using this configuration sufficiently reproduces both the absolute heave measured by geodetic leveling and the relative displacements from the hose levels (Kostadinovic, 2023).

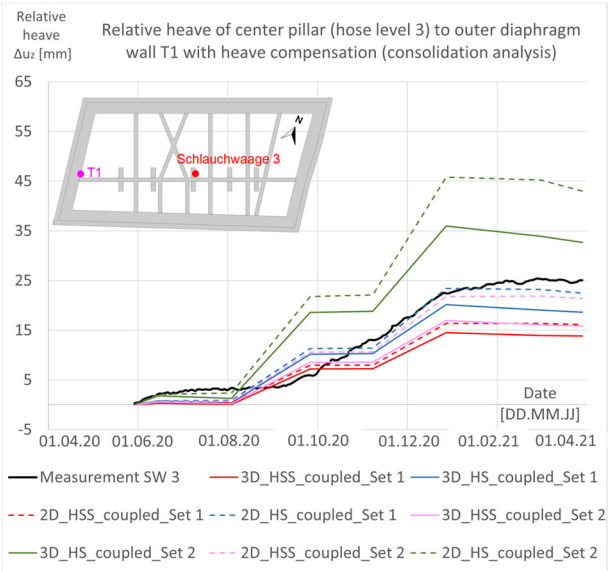

Figure 6. Relative elevations of the temporary pillar around the water level gauge 3; comparison between the measured data and the calculation results from the consolidation analysis (Kostadinovic, 2023).

4.4 *Effect of different pre-over-burden-pressures on the calculation results*

The geological preload is an important parameter for fine-grained, overconsolidated soils. It provides information about the prehistoric overburden stress to which a soil was exposed. The pre-overburden pressure (POP) can be used to quantify this preload and precisely indicates the vertical overburden stress described above. The POP is considered as an input parameter in the finite element calculation and influences the deformation behavior of the diaphragm wall shaft.

To investigate the influence of the POP both on the horizontal deformations of the outer diaphragm wall and on the heave of the excavation base, the POP is varied between 0 kN/m² and 1600 kN/m² and compared with the results of the reference model with POP = 800 kN/m². Figure 7 shows the horizontal diaphragm wall deformations calculated in the course of the soil parameter study. If the POP is neglected or set to zero in the calculation model (red line), up to 21 % greater horizontal deformations of the diaphragm walls are calculated. Overestimating the POP, on the other hand, does not lead to any significant deviations in the results. Halving or doubling the POP only results in 5 % larger or smaller diaphragm wall deformations. The diaphragm wall deformations based on POP = 1200 kN/m² (green line) and POP = 1600 kN/m² (blue line) differ only slightly.

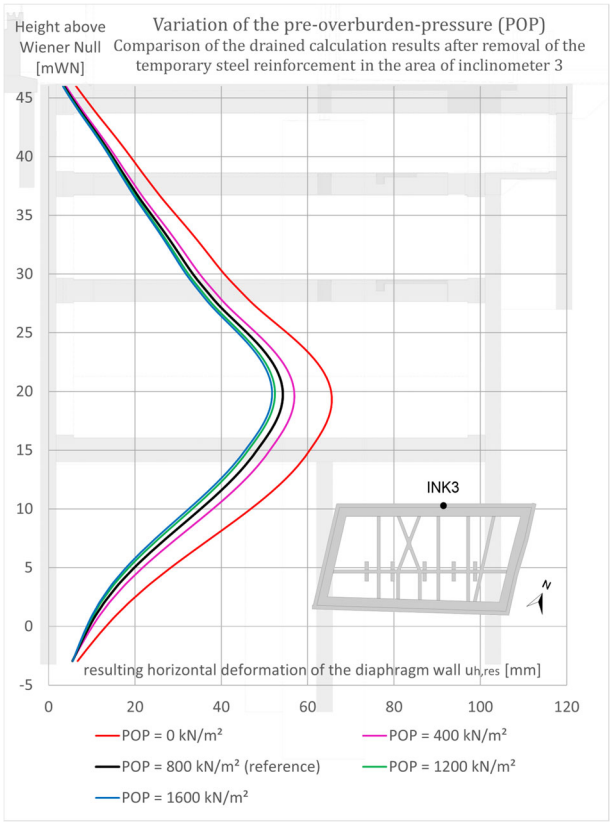

Figure 7. Effect of the variation of the pre-overburden pressure (POP) of the Miocene layers on the horizontal diaphragm wall deformations (Kostadinovic, 2023).

Neglecting the POP in the calculation model leads to larger calculated diaphragm wall deformations, whereas overestimating the POP does not result in significantly smaller diaphragm wall deformations. If there is no POP as an input parameter in the calculation model for over-consolidated soils available, it is generally better to roughly estimate the POP than to disregard it completely.

4.5 *Axial force of the temporary steel bracing*

To further validate the suitability of the FE calculation models the axial forces recorded by the load monitoring of the hydraulic steel struts are also compared with the calculation results. The measurement results of steel strut No. 19 (highlighted in red in figure 8) are used to compare the measured strut forces with the results of the FE calculation.

Figure 8 shows the comparison between the calculation results from the consolidation analysis and the monitored strut forces of hydraulic strut No. 19. The measured strut force exceeds all calculated values. Additionally, the calculations of the 2D models (dashed lines) result in strut forces that are nearly twice as high as those of the 3D models (solid lines). This discrepancy is due to planar calculations, which cannot account for spatial effects such as the stiff corners of the shaft. The strut forces calculated using the 3D-HSS model with Soil Parameter Set 1 (red solid line) most closely resemble the measured results (Kostadinovic, 2023).

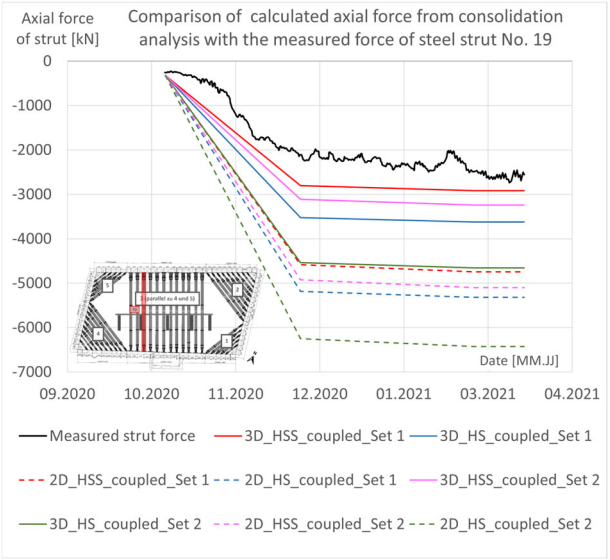

Figure 8. Axial force of the hydraulic strut No. 19; comparison between the measured strut forces and the calculation results from the consolidation analysis (Kostadinovic, 2023).

5 CONCLUSION

The numerical analyses demonstrate that calculated diaphragm wall deformations and excavation base heave are significantly influenced by the constitutive model, the soil parameter derivation method and the drainage condition type.

3D-HSS models using Soil Parameter Set 1, which is derived from in situ self-drilling pressuremeter tests, consistently underpredict measured diaphragm wall deformations and excavation base heave. This discrepancy may be due to the partially drained conditions during the field tests, as these conditions can affect the determined soil stiffness. In contrast, the 3D-HS models with Set 1 slightly overestimate the measured deformations. This overestimation results from the omission of the small-strain-stiffness-effect, which plays a crucial role in accurately modeling the deformation behavior of stiff soils at low strain levels.

Comparative analyses of the HS and HSS models show that the HSS model produces smaller diaphragm wall deformations and significantly lower base heave than the HS model for all configurations. Neglecting the small-strain-stiffness-effect increases diaphragm wall deformations by up to 149 % and excavation base heave by up to 385 %, depending on the model configuration.

As expected, 2D models predict larger deformations than 3D models because plane-strain conditions do not permit three-dimensional stress redistribution, such as stiff shaft corners or spatial load dispersion. Furthermore, drained analyses consistently result in higher calculated base heave than undrained and consolidation analyses. This difference is primarily caused by the generation of negative excess pore water pressures during the excavation process, which counteracts basal heave.

The 3D-HSS model with Soil Parameter Set 2 (derived from laboratory tests) under consolidation conditions produced the best agreement between calculated and measured values in terms of both diaphragm wall deformation and basal heave. This configuration captures the effects of time-dependent pore pressure dissipation and includes the small-strain stiffness response, which is essential for modeling low-strain soil behavior.

The parameter study showed that if the POP is neglected or set to zero in the calculation model, up to 21 % larger horizontal deformations of the diaphragm walls were calculated. Overestimating the POP, on the other hand, did not lead to any significantly high deviations in the calculation results compared to the wall deformations calculated in the reference model. If no POP is available, it is still better to roughly estimate the POP than to neglect it completely, as otherwise too large deformations are calculated.

The results highlight the importance of accurate soil parameter determination for the reliable application of advanced constitutive models in finite element simulations. Although field tests such as self-drilling pressuremeter tests offer a promising basis for parameter derivation, it is crucial to account for drainage conditions during test execution, especially when calibrating constitutive soil models.

In conclusion, the broader implementation of finite element methods in geotechnical design requires the availability of well-calibrated, high-quality material parameters. These parameters must be validated through numerical back-analyses and comparative studies to ensure reliability (Kostadinovic, 2023).

6 ACKNOWLEDGEMENTS

The authors would like to thank Wiener Linien and the Municipal Department 29 of the City of Vienna (MA 29), Division of Geotechnical Engineering, for providing the project documents and monitoring data for the U2-U5 Matzleinsdorfer Platz construction project.

7 REFERENCES

Alpan, I., 1970. The geotechnical properties of soils. *Earth-Science Reviews* 6, 5–49. https://doi.org/10.1016/0012-8252(70)90001-2

Ampera, B., Aydogmus, T., 2005. Skin Friction between Peat and Silt Soils with Construction Materials. *Electronic Journal of Geotechnical Engineering* 10.

Benz, T., 2007. *Small-strain stiffness of soils and its numerical consequences* (Dissertation). Mitteilung des Instituts für Geotechnik 55. IGS, Stuttgart.

Benz, T., Schwab, R., Vermeer, P., 2007. Zur Berücksichtigung des Bereichs kleiner Dehnungen in geotechnischen Berechnungen. *Bautechnik* 84, 749–761. https://doi.org/10.1002/bate.200710063

Biarez, J., Hicher, P.Y., 1994. *Elementary Mechanics of Soil Behaviour: Saturated Remoulded Soils*. A.A. Balkema.

Bode, M., Schranz, F., Medicus, G., Fellin, W., 2019. Vergleich unterschiedlicher Materialmodelle an einer Aushubsimulation. *Geotechnik* 42, 11–20. https://doi.org/10.1002/gete.201800016

Burd, H., Dong, Y., Houlsby, G., 2016. Finite-element analysis of a deep excavation case history. *Géotechnique* 66, 1–15. https://doi.org/10.1680/geot.14.P.234

Chowdhury, S., Deb, K., Sengupta, A., 2013. Estimation of Design Parameters for Braced Excavation: Numerical Study. *International Journal of Geomechanics* 13. https://doi.org/10.1061/(ASCE)GM.1943-5622.0000207

Deutsche Gesellschaft für Geotechnik, 2014. *Empfehlungen des Arbeitskreises Numerik in der Geotechnik – EANG.* John Wiley & Sons, Ltd. https://doi.org/10.1002/9783433604489.fmatter

Dong, Y.P., Burd, H.J., Houlsby, G.T., 2015. Finite-element analysis of a deep excavation case history. *Géotechnique* 66, 1–15. https://doi.org/10.1680/jgeot.14.P.234

European Comittee for Standardization, 2014. *ÖNORM EN 1997–1, Eurocode 7: Entwurf, Berechnung und Bemessung in der Geotechnik – Teil 1: Allgemeine Regeln (konsolidierte Fassung).* Brussels: CEN.

Hardin, B.O., Drnevich, V.P., 1972. Shear Modulus and Damping in Soils: Design Equations and Curves. *Journal of the Soil Mechanics and Foundations Division* 98, 667–692. https://doi.org/10.1061/JSFEAQ.0001760

Houhou, M.N., Emeriault, F., Belounar, A., 2019. Three-dimensional numerical back-analysis of a monitored deep excavation retained by strutted diaphragm walls. *Tunnelling and Underground Space Technology* 83, 153–164. https://doi.org/10.1016/j.tust.2018.09.013

Klein, L., Moormann, C., 2017. Beitrag zur Abbildung von Schlitzwänden in räumlichen Finite-Elemente-Berechnungen. *Bautechnik* 94, 559–578. https://doi.org/10.1002/bate.201700016

Kostadinovic, A., 2023. *Numerische Modellierung eines tiefen Schlitzwandschachtes im überkonsolidierten Boden des Wiener Raums* (Thesis). Technische Universität Wien.

Kostadinovic, A., Sigmund, J., Adam, D., 2024. Numerische Modellierung eines tiefen Schlitzwandschachtes im überkonsolidierten Boden des Wiener Raums. *Bauingenieur* 99, 123–137. https://doi.org/10.37544/0005-6650-2024-04-55

Law, K.H., Hashim, R., Ismail, Z., 2014. 3D numerical analysis and performance of deep excavations in Kenny Hill formation. *1st MGS-GeoSS Conference,* Kuala Lumpur, Malaysia. https://doi.org/10.1201/b17017-136

Melnikov, R., Zazulya, J., Stepanov, M., Ashikhmin, O., Maltseva, T., 2016. OCR and POP Parameters in Plaxis-based Numerical Analysis of Loaded over Consolidated Soils. Procedia Engineering, *15th International scientific conference "Underground Urbanisation as a Prerequisite for Sustainable Development"* 12-15 September 2016, St. Petersburg, Russia, 845–852. https://doi.org/10.1016/j.proeng.2016.11.783

Potyondy, J.G., 1961. Skin Friction between Various Soils and Construction Materials. *Géotechnique* 11, 339–353. https://doi.org/10.1680/geot.1961.11.4.339

Schanz, T., 1998. Zur Modellierung des mechanischen Verhaltens von Reibungsmaterialien.

Schweiger, H.F., Vermeer, P.A., Wehnert, M., 2009. On the design of deep excavations based on finite element analysis. *Geomechanics and Tunnelling* 2, 333–344. https://doi.org/10.1002/geot.200900028

Stokoe, K.H., Darendeli, M.B., Gilbert, R.B., 2004. Development of a new family of normalized modulus reduction and material damping curves. Presented at the *Int. Workshop on Uncertainties in Nonlinear Soil Properties and their Impact on Modelling Dynamic Soil Response*, Berkley.

Vucetic Mladen, Dobry Ricardo, 1991. Effect of Soil Plasticity on Cyclic Response. *Journal of Geotechnical Engineering* 117, 89–107. https://doi.org/10.1061/(ASCE)0733-9410(1991)117:1(89)

Wichtmann, T., Triantafyllidis, T., 2006. Über die Korrelation der ödometrischen und der "dynamischen" Steifigkeit nichtbindiger Böden. *Bautechnik* 83, 482–491. https://doi.org/10.1002/bate.200610041

Zdravkovic, L., John, H., Potts, D., 2005. Modelling of a 3D excavation in finite element analysis. *Geotechnique* 55, 497–513. https://doi.org/10.1680/geot.2005.55.7.497

Zhang, W., Liu, H., 2022. *Design of Deep Braced Excavation and Earth Retaining Systems Under Complex Built Environment: Theories and Case Studies*. Springer, Singapore. https://doi.org/10.1007/978-981-16-5320-9